Hindawi Publishing Corporation
Mathematical Problems in Engineering
Volume 2016, Article ID 5967159, 13 pages
http://dx.doi.org/10.1155/2016/5967159

Research Article

Characterization of Rock Mechanical Properties Using Lab Tests and Numerical Interpretation Model of Well Logs

Hao Xu,[1] Wen Zhou,[1] Runcheng Xie,[1] Lina Da,[2] Christopher Xiao,[3] Yuming Shan,[1] and Haotian Zhang[1]

[1]*State Key Laboratory of Oil and Gas Reservoir Geology and Exploitation, Chengdu University of Technology, Chengdu 610059, China*
[2]*The Pennsylvania State University, University Park, PA 19019, USA*
[3]*University of Houston, Houston, TX 77004, USA*

Correspondence should be addressed to Wen Zhou; Zhouw62@cut.edu.cn and Runcheng Xie; xieruncheng@cdut.cn

Received 25 November 2015; Revised 18 March 2016; Accepted 3 April 2016

Academic Editor: Gregory Chagnon

The tight gas reservoir in the fifth member of the Xujiahe formation contains heterogeneous interlayers of sandstone and shale that are low in both porosity and permeability. Elastic characteristics of sandstone and shale are analyzed in this study based on petrophysics tests. The tests indicate that sandstone and mudstone samples have different stress-strain relationships. The rock tends to exhibit elastic-plastic deformation. The compressive strength correlates with confinement pressure and elastic modulus. The results based on thin-bed log interpretation match dynamic Young's modulus and Poisson's ratio predicted by theory. The compressive strength is calculated from density, elastic impedance, and clay contents. The tensile strength is calibrated using compressive strength. Shear strength is calculated with an empirical formula. Finally, log interpretation of rock mechanical properties is performed on the fifth member of the Xujiahe formation. Natural fractures in downhole cores and rock microscopic failure in the samples in the cross section demonstrate that tensile fractures were primarily observed in sandstone, and shear fractures can be observed in both mudstone and sandstone. Based on different elasticity and plasticity of different rocks, as well as the characteristics of natural fractures, a fracture propagation model was built.

1. Introduction

Quantitative characterization of rock mechanical properties is critical for reservoir exploitation, including the design of proper drilling, well completion, and production programs [1, 2]. Rock mechanical properties, such as compressive strength, Young's modulus, and Poisson's ratio, play an important role in wellbore stability, fracture prediction, and other engineering techniques [3, 4]. Mechanical properties of rocks are usually measured using static and dynamic methods [1, 5]. Static methods are generally conducted in the lab with specific test equipment that contains core specimens [6]. The specimens are continuously compressed until failure occurs. Stress-strain curves are simultaneously recorded using a computer and mechanical parameters can be obtained from the curves. Dynamic methods are usually calculations of compressional wave velocities (VP) and shear wave velocities (VS), which can be obtained from logs or in the lab [2, 7–9]. Abundant studies regarding the differences between static and dynamic methods have demonstrated that static methods are more direct and realistic, while dynamic methods are easier and more continuous [3, 10, 11]. Therefore, comprehensive data on rock mechanical properties is needed both from lab experiments and from well logs. The very first use of empirical relations based on well logs to acquire rock mechanical parameters dates back to 1963 [12]. Many people have tried to modify the empirical relations thereafter for different geological areas with different depositional settings [13–15].

The geological conditions in the Sichuan Basin are favorable for the development of shale gas reservoirs. The Sichuan Basin has shale gas resources with the best quality and largest recoverable volume. China's first successful shale gas field, known as Changning-Weiyuan, is located in the Sichuan Basin [16]. SINOPEC reported that the Fuling shale gas field

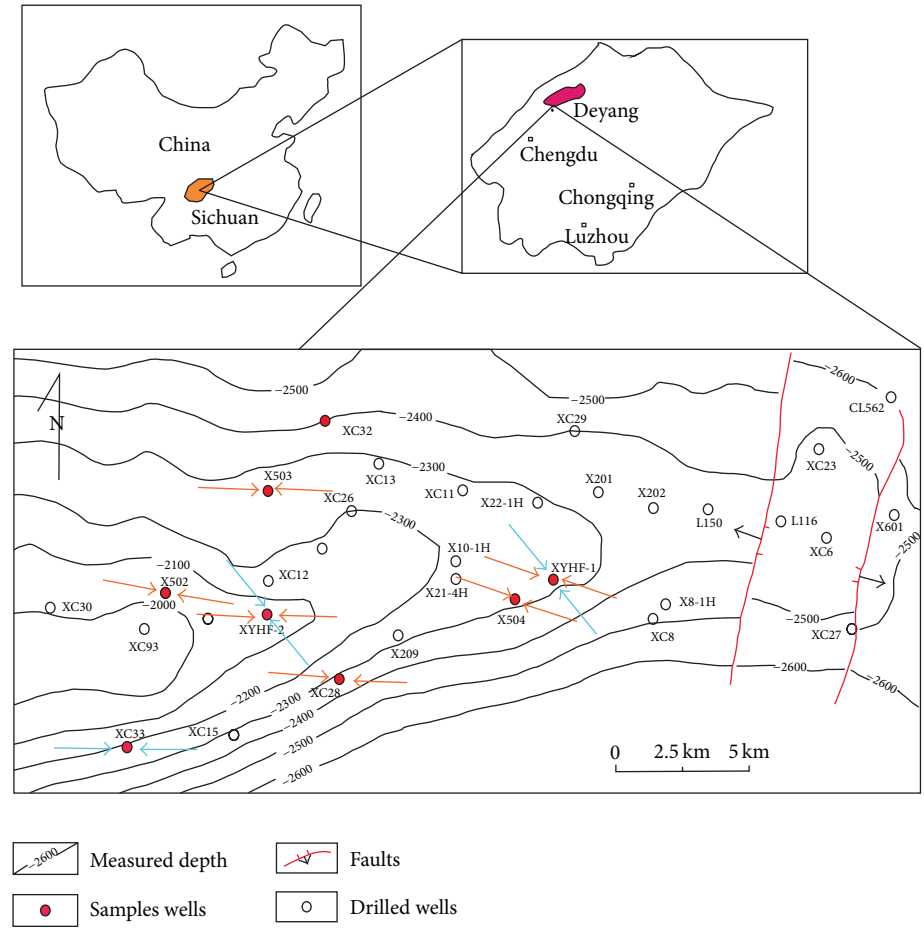

FIGURE 1: Contour map of the research area. The two faults are shown as red lines. The wells are marked by circles. The inset indicates the research area in the northwest of the Sichuan Basin. Orange arrows represent stress direction interpreted by imaging logging. Blue arrows represent stress direction interpreted by paleomagnetism.

in the southeast of Sichuan Basin has explored reserves of 3806×10^8 m^3. The fifth member of the Xujiahe formation, a new horizon, is considered as tight sand-shale interbedded reservoir with high potential production [17]. However, fundamental investigation is lacking, including data on stress distribution and fracture propagation. The study of rock mechanical characteristics is therefore particularly important.

In this paper, many empirical relations based on laboratory experiments and well logs have been studied for characterization analysis of rock mechanical properties [3, 13, 14]. For the first time, the fifth member of the Xujiahe formation of the Xinchang gas field in western China has been studied. This research plays an essential role in the calculation of in situ stress and the design of drilling and hydraulic fracturing.

2. Geological Conditions of the Research Area

The research area is located in the western Sichuan Basin in southwestern China. More than 100 wells are producing in this area. The highest producing well, called X851, can reach 151.7×10^4 m^3 per day. In addition, the well has shown good shale gas production. More than six wells (e.g., X32, X26, XYHF-1, X33, and X503) were drilled for unconventional gas exploitation in this area. These wells showed good test production (up to 7.78 m^3/day) before hydraulic fracturing (data from SINOPEC). The test production indicates that the formation is a very good target for gas production by hydraulic fracturing. Therefore, we carry out this study to characterize the rock mechanical properties as a prerequisite for hydraulic fracturing.

Many scientists have undertaken considerable research investigating stress tests. There are many ways to obtain stress data, such as hydraulic fracturing, well logs, and seismic focal plane mechanisms [18–20]. Barton and Zoback [21] believe wellbore-imaging logs can efficiently determine the stress direction. In this study, imaging logs and paleomagnetism were used to determine the stress direction. The structure is mainly oriented in the NEE direction, while the current stress is acting mainly EW. Two faults cross the east of the study area (Figure 1).

The Xujiahe formation is the main reservoir for the Upper Triassic gas system, and the fifth member of the Xujiahe formation is the main source rock, composed of

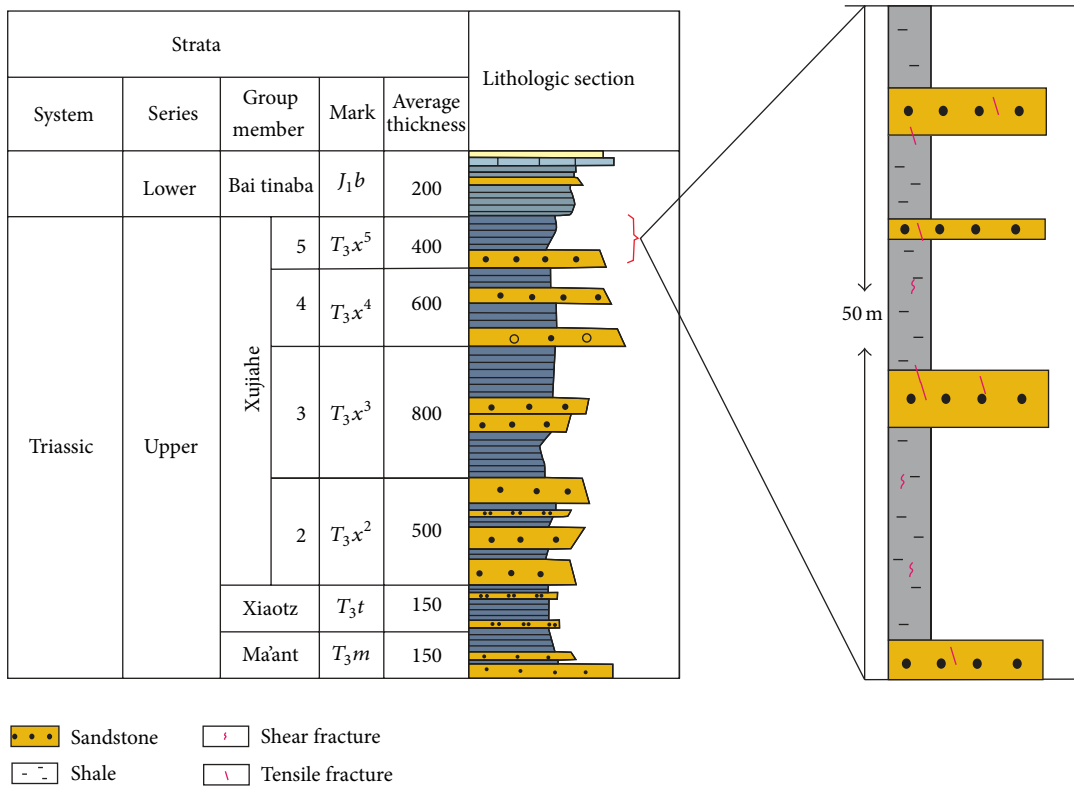

Figure 2: Illustration of the 5th member of the Xujiahe formation.

black shale, grey mudstone, and sandstone. The measured depth of the formation is approximately 3000 m, and the formation is approximately 400 m in thickness. Figure 2 shows that the 5th member of the Xujiahe formation is a tight sand-shale interbedded reservoir. Unlike common shale gas reservoirs, the shale is separated by sandstone and the shale strata are not continuous. Therefore, it is essential to analyze the differences of mechanical properties of sandstone and shale. Additionally, different empirical correlations should be used to predict Young's modulus, Poisson's ratio, and compressive strength. This might improve accuracy and the log interpretation might be more reliable.

3. Static Rock Mechanical Properties from Laboratory Experiments

3.1. Equipment and Samples. Laboratory data are a direct and efficient means of investigating rock mechanical properties [1, 22]. In order to evaluate rock mechanical properties comprehensively, many direct experiments have been carried out in the laboratory. All of the experiments of this study were carried in the State Key Laboratory of Oil and Gas Reservoir Geology and Exploration, including tensile strength tests, uniaxial compression tests, triaxial compression tests, and shear tests. The main test system is MTS (Mechanics Test System) as shown in Figure 3. This system can simulate underground conditions with an axial pressure of up to 1000 kN, a confining pressure of up to 140 MPa, and a temperature of up to 200°C. In addition, samples can be saturated with oil or water. Stress and displacement signals can be obtained automatically with a Teststar digital controller. Generally, it can output stress-strain curve, S-wave, and P-wave. With these data, Young's modulus, Poisson's ratio, and the compressive strength can be easily calculated. The test system requires samples to be 25 mm in diameter and 50 mm in length. In this study, experimental core samples (both sandstone and mudstone) of the fifth member of the Xujiahe formation were collected from 6 wells at depths ranging from 3,055.53 m to 3,393.3 m.

3.2. Deformation Characteristics of Sandstone and Mudstone under Different Confining Pressures. Deformation characteristics of rocks are mainly related to the rock type. The characteristics of deformation are quite different under different confining pressures [23]. Two groups of sandstone and mudstone core samples were collected at the same depth of the same well, that is, from approximately the same subsurface conditions. The same tests were carried out at a temperature of 25°C and water saturation. The stress-strain curves of these two groups are shown in Figure 4. It is notable that different types of rocks have divergent mechanical properties. Figure 4 shows the axial strain of sandstone and mudstone under various axial differential stresses. The compressive strength of sandstone is higher than that of mudstone under

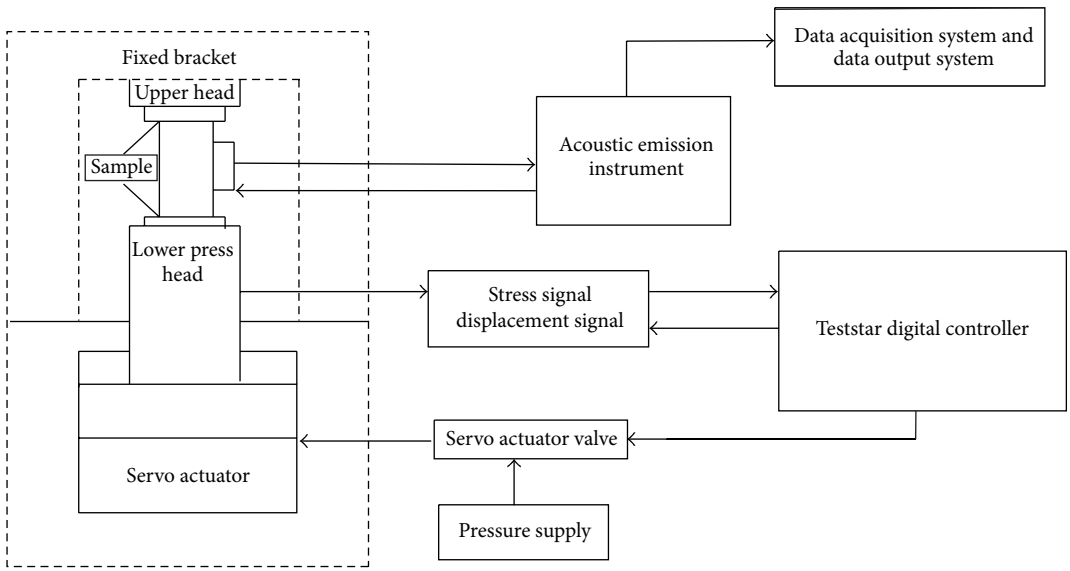

Figure 3: The Mechanics Test System.

Table 1: Experimental rock mechanical properties (effective confining pressure: 32 MPa, temperature: 25°, saturated with water).

Lithology	Value	Compressive strength (Mpa)	Young's modulus (Gpa)	Poisson's ratio
Sandstone	Maximum	273.13	58.5	0.487
	Minimum	111.0	17.7	0.086
	Average	191.51	36.36	0.272
Mudstone	Maximum	128.38	34.86	0.438
	Minimum	73.94	17.41	0.238
	Average	106.99	23.82	0.329

the same confining pressure. The rock compressive strength increases with changing confining pressures for sandstone and mudstone.

Under uniaxial conditions, the rock first shows signs of compaction followed by transition to elastic deformation. The main deformation mode is brittle deformation.

Under three-dimensional stress, the rock tends to exhibit elastic-plastic deformation. The higher the confining pressure is, the greater the degree of plastic deformation is. The main failure mode is shear deformation. In addition, sandstones show strong rigidity, while mudstones show plasticity.

3.3. Elastic Modulus and Compressive Strength of Sandstone and Mudstone. (1) Fifteen core samples were used to conduct rock mechanical tests. Firstly, samples were required to be saturated with water before test. The test temperature was 25°C. The rock mechanical parameters under three-dimensional stresses acquired from experiments are listed in Table 1. Compressive strength conditions in the laboratory are similar to those of the subsurface (32 MPa, water-saturated). The experimental results (Table 1) show that compressive strength and elastic modulus of sandstone are notably higher than those of the mudstone and that Poisson's ratio is lower than that of the mudstone. This indicates that the mudstone is more plastic, while the sandstone is more rigid. In addition, Young's modulus of sandstone under uniaxial pressure ranges from 11.3 to 40 GPa with an average value of 19.9 GPa. Static Poisson's ratio ranges from 0.279 to 0.489 with an average value of 0.373 GPa. It is very clear that Young's modulus of sandstone is significantly higher under uniaxial pressure than under three-dimensional stress, while static Poisson's ratio is higher under uniaxial pressure.

(2) A strong correlation exists between compressive strength and Young's modulus, and the correlation differs for sandstone and mudstone (Figure 5). Accordingly, compressive strength can be calculated from corresponding Young's modulus considering lithology composition when there is a lack of lab measurements. The compressive strength of sandstone increases rapidly with Young's modulus, while the compressive strength of mudstone increases relatively slow. At the same high elastic modulus, the compressive strength of sandstone is bigger than that of mudstone. Hence, it is very possible that shear fractures in the sandstone layer can penetrate the interface between the sandstone layer and the mudstone layer. Even interlayer or space network fractures may be developed.

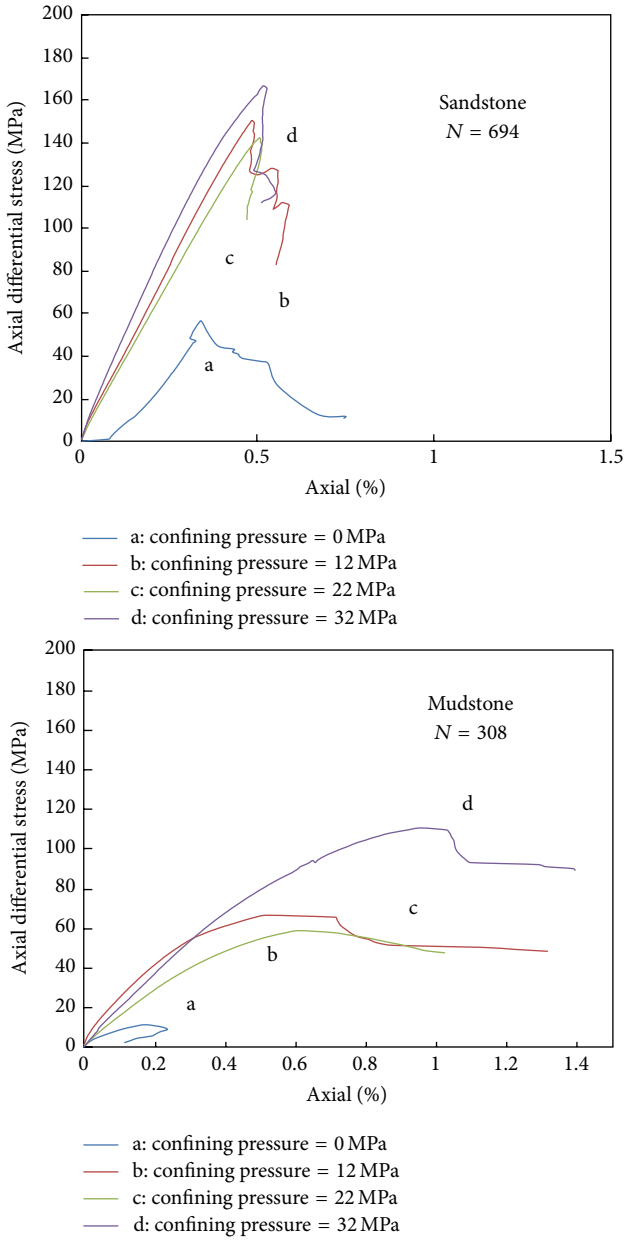

Figure 4: The stress-strain relation of sandstone and mudstone under different confining pressures.

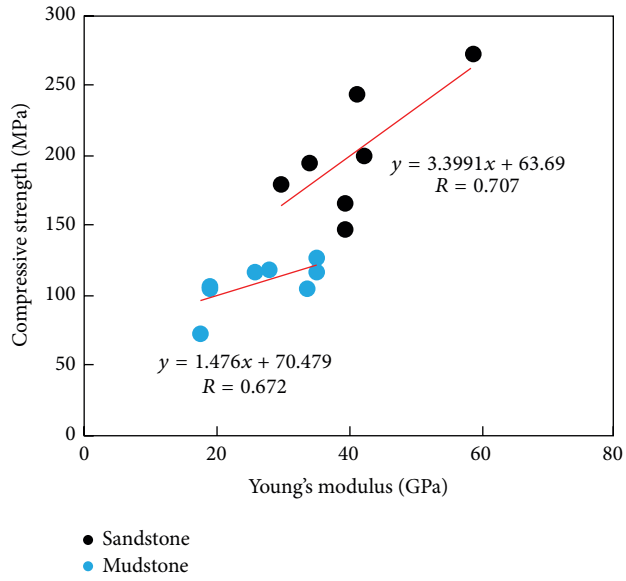

Figure 5: Relationship between compressive strength and elastic modulus.

4. Determining Rock Mechanical Properties from Log Interpretation

4.1. Calculation of Transverse Slowness. Figure 6 shows the characteristic linear relationships between S-wave transverse slowness and P-wave compressional slowness of sandstone and mudstone from wells CX565 and Lian150. Because S-wave slowness is often absent in conventional logging data, P-wave slowness can be used to approximate S-wave slowness when the composition is known.

4.2. Calculation of Dynamic Modulus. Dynamic Young's modulus and Poisson's ratio can be calculated using longitudinal slowness, transverse slowness, and bulk density data. Young's modulus and Poisson's ratio are usually obtained using the following well-known equations:

Young's modulus:

$$E_d = \left(\frac{\rho_b}{\Delta t_s^2}\right)\left(\frac{3\Delta t_s^2 - 4\Delta t_p^2}{\Delta t_s^2 - \Delta t_p^2}\right) \times 10^{-6}; \quad (1)$$

Poisson's ratio:

$$\mu = \frac{1}{2}\left(\frac{\Delta t_s^2 - 2\Delta t_p^2}{\Delta t_s^2 - \Delta t_p^2}\right), \quad (2)$$

where Δt_p is compression slowness, μs/m; Δt_s is transverse slowness, μs/m; ρ_b is density, g/cm^3; E is Young's modulus, MPa; μ is Poisson's ratio.

4.3. Conversion from Dynamic Moduli to Static Moduli. Dynamic moduli derived from well log data are different from static moduli. Static mechanical parameters are more in line with the actual engineering needs because they represent the rock deformation under the high stresses of subsurface conditions. When static mechanical moduli measurements are not available in the laboratory, it is necessary to convert dynamic to static parameters. Figure 7 shows the experimental relation between static and dynamic Poisson's ratio and the relation between static and dynamic Young's modulus of sandstone and mudstone. Linear conversions are used in this study.

4.4. Calculation of Compressive Strength and Tensile Strength. (1) Under formation conditions, the compressive strength of the rock increases with rock density and decreases with rock porosity (Figure 8).

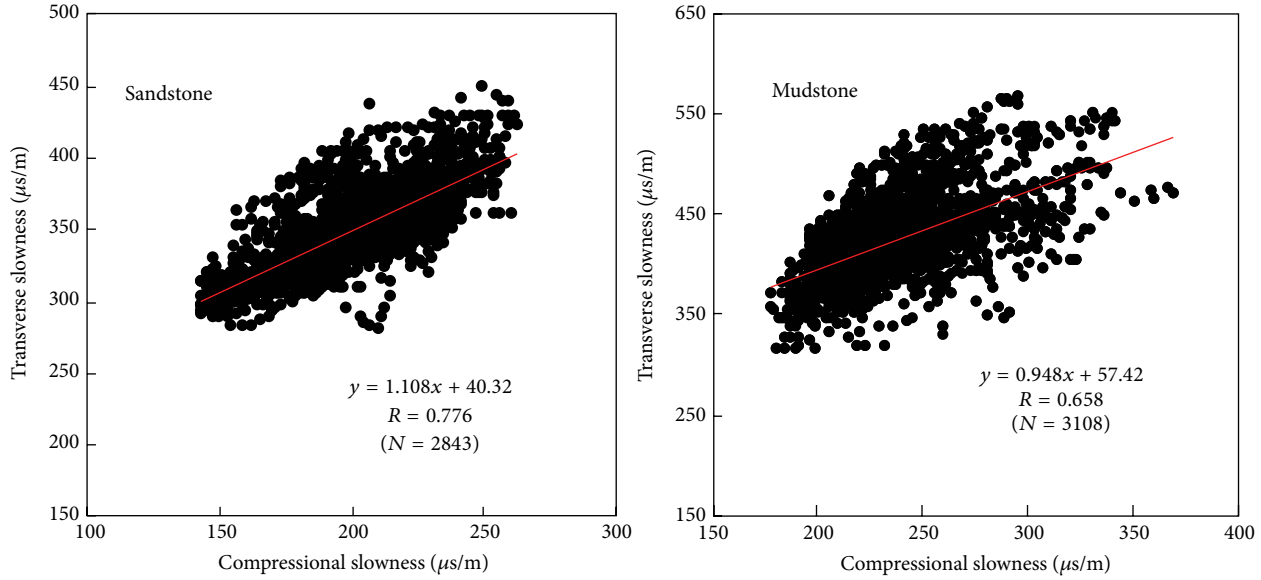

Figure 6: Relation between S- and P-waves of the sandstone and the mudstone.

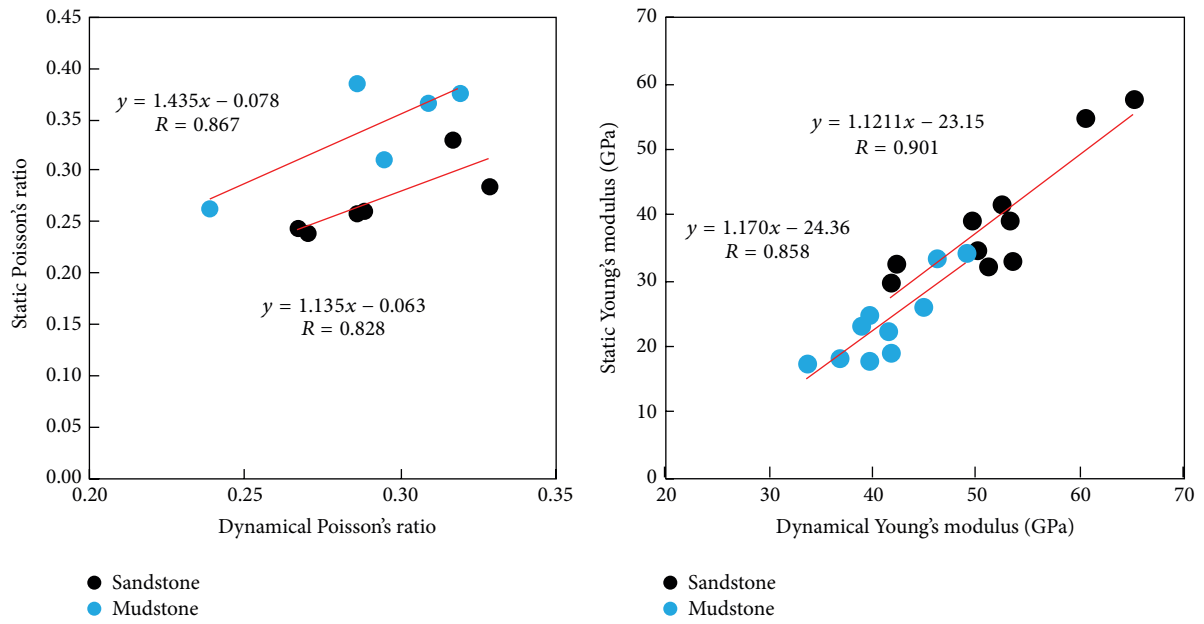

Figure 7: Dynamic and static conversion of Poisson's ratio and Young's modulus.

(2) Compressive strength and tensile strength are closely related to such factors as the mineral composition and porosity distribution. The compressive strength can be directly obtained in the lab or calculated from other data, such as well logging data. Many possible parameters, including density, gamma ray, clay content, resistivity, and wave impedance, have been used in this paper to calculate the compressive strength. The figures (e.g., Figure 9) demonstrate good relationships. Hence, the method is reliable.

Static rock mechanical characteristics were derived by analysis of mechanical parameters of sandstone and mudstone rock samples. Dynamic parameters were later obtained using acoustic logging data, as well as density, gamma ray, clay index, resistivity, acoustic impedance, and other data. Finally, a rock mechanical log interpretation model of the fifth member of Xujiahe formation was built for longitudinal section distribution.

(3) Figure 9 shows that the compressive strength of the rock is positively correlated with the P-wave and wave impedance and negatively correlated with clay content and mud index. Therefore, the best method to calculate compressive strength is using [(wave impedance)^2/mud index]. It is observed that the linear correlation between triaxial compressive strength of the rock and [(wave impedance)^2/mud index]

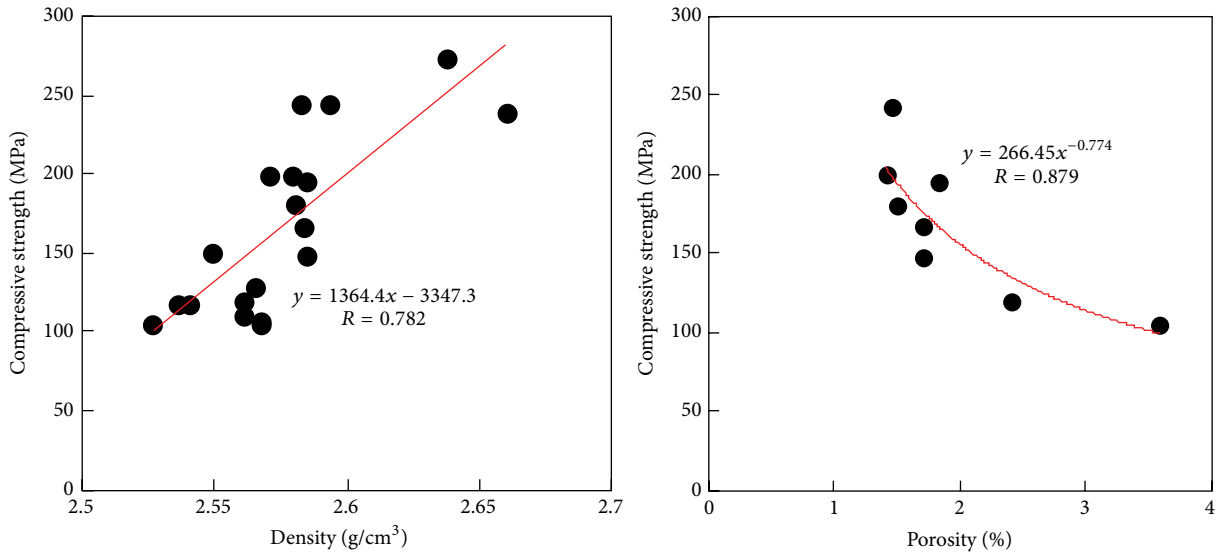

Figure 8: Relation between compressive strength and density and porosity under saturated formation conditions.

is the strongest: sandstone: $y = 1.168x + 22.01.7$; $R = 0.841$; mudstone: $y = 1.212x + 30.90$; $R = 0.846$ (y stands for compressive strength; x stands for [(wave impedance)^2/mud index]). The tensile deformation mechanism of the rock is similar to the compressive deformation mechanism. The experimental data shows a good linear correlation: $y = 0.029x + 0.17$, $R = 0.820$ (y stands for tensile strength; x stands for compressive strength).

4.5. Calculation of Cohesion Force and Internal Friction Angle. Coates and Denoo [24] and Bruce [25] summarized the empirical formula of shear strength. In combination with the characteristics of the Xujiahe formation, the modified empirical formula of cohesion force and internal friction angle can be obtained as follows.

Sandstone:

$$C = 19.19 - 2.1923 \times 10^{13} \rho_b^2 \left(\frac{1+\nu_d}{1-\nu_d}\right)(1-2\nu_d)\frac{(1+0.78V_{sh})}{\Delta t_p^4},$$
$$M = 0.16 - 0.197 \cdot C,$$
$$\phi = 48.88 - 11.43 \lg\left[M + \left(M^2+1\right)^{0.5}\right]. \quad (3)$$

Mudstone:

$$C = 6.944 - 0.2957 \times 10^{13} \rho_b^2 \left(\frac{1+\nu_d}{1-\nu_d}\right)(1-2\nu_d)\frac{(1+0.78V_{sh})}{\Delta t_p^4},$$
$$M = 0.16 - 0.197 \cdot C,$$
$$\phi = 35.43 - 14.46 \lg\left[M + \left(M^2+1\right)^{0.5}\right], \quad (4)$$

Table 2: The comparison of experimental and calculated petrophysical parameters.

Petrophysical parameter	Lithology	Experimental data	Calculated data
Compressive strength	Sandstone	111.0~273.13 MPa	150~350 MPa
	Mudstone	73.94~128.38 MPa	90~200 MPa
Young's modulus	Sandstone	17.70~58.8 GPa	35~60 GPa
	Mudstone	17.41~34.86 GPa	25~40 GPa
Poisson's ratio	Sandstone	0.086~0.487	0.16~0.28
	Mudstone	0.238~0.438	0.12~0.24
Cohesive force	Sandstone	9~19 MPa	10~20 MPa
	Mudstone	5~13 MPa	4~12 MPa

where C is cohesion force, MPa; ϕ is internal friction angle, °; μ_d is Poisson's ratio; V_{sh} is clay content; ρ_b is bulk density, g/cm^3; Δt_p is compressional slowness, μs/m.

5. Log Interpretation Section of Rock Mechanical Parameters

The log or laboratory measured data directly reflects rock mechanical properties, but it is not possible for all regions of all intervals to be measured sequentially due to the high engineering cost and operation complexity. Therefore, the establishment of the whole well rock mechanics parameter logging interpretation section is significant and is worth further study. The log interpretation section is established based on conventional logging data, rock mechanics parameters, and prediction formula (Figure 10).

From log interpretation, longitudinal distribution of rock mechanical properties is obtained, which can help in hydraulic fracturing design and new well drilling. Log-calculated mechanical rock properties and measured data are compared in Table 2. The comparison shows that the static method from lab tests and the dynamical method give similar results. The logging predictions of compressive strength and

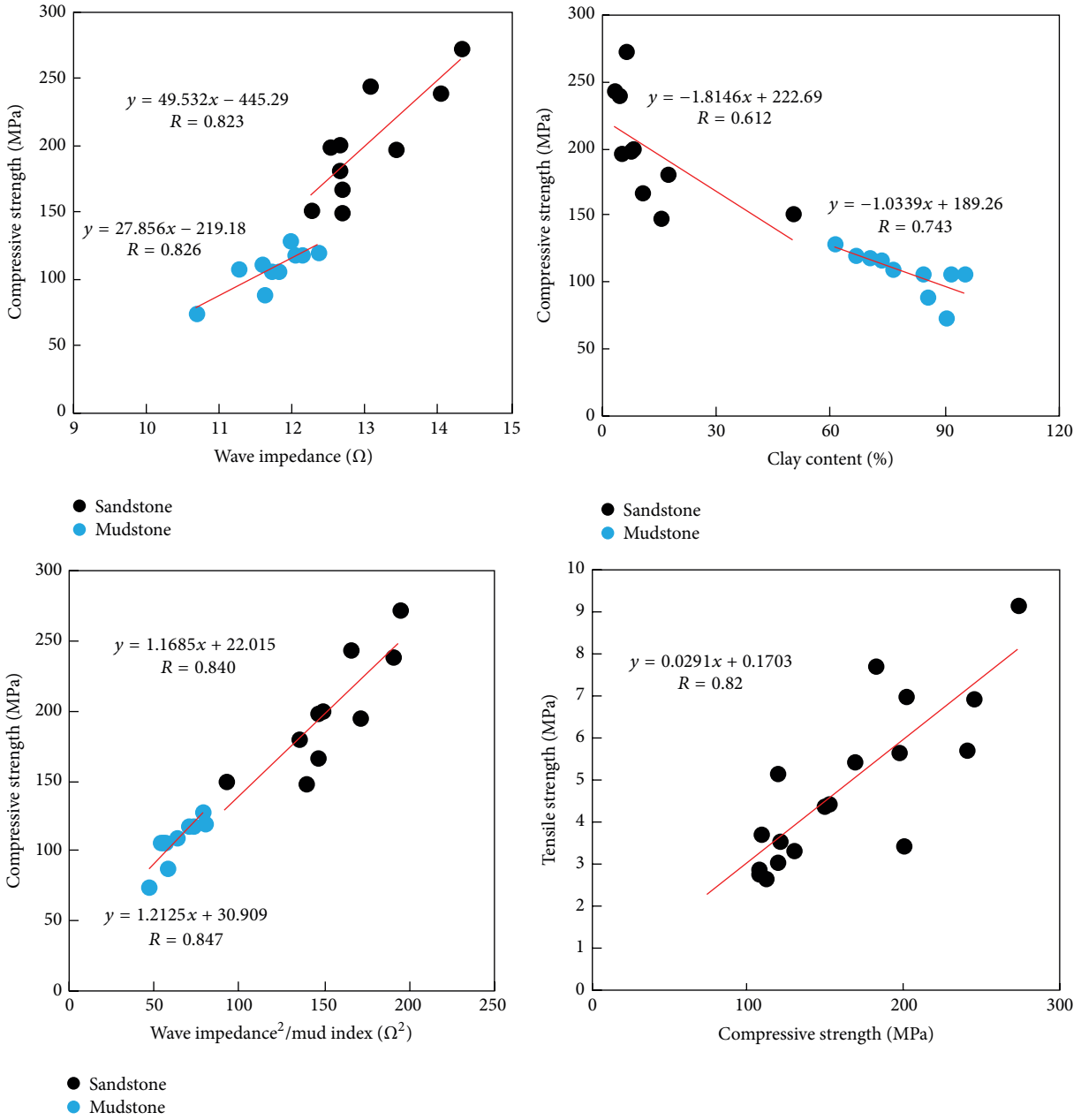

Figure 9: The relationship between compressive strength and P-wave, clay content, mud index, and wave impedance.

cohesive force are very close to the respective measured data. The error of compressive strength and cohesion is limited, and the log interpretation method is reliable. However, the calculated Young's modulus is larger than that of the measured data. The calculated Poisson's ratio is lower than the measured value. Possible causes for these differences can be improper derived transverse slowness and inaccurate formula from limited experimental data.

6. Natural Fractures and Rock Microscopic Failure

6.1. Natural Fractures. Eighty-one natural fractures were found in downhole cores from six wells (XC28, XC33, XC32, X503, XYHF-1, and XYHF-2). The width of fractures ranged from 0 to 0.5 mm. Most natural fractures are tensile fractures and shear fractures. Ninety percent of natural fractures were found in sandstone and shale (Figure 11).

6.2. Microscopic Failures. Several types of microscopic failures were observed in samples of the cross section. The width of these microscopic failures ranged from 0.01 to 0.05 mm. There were two main fractures: tensile fractures and shear fractures. Tensile fractures were mainly found in sandstone; meanwhile, dissolution usually accompanied tensile fractures (Figure 12(a)). While shear fractures were mainly found in mudstone, "X" type fractures could be found in mudstone as

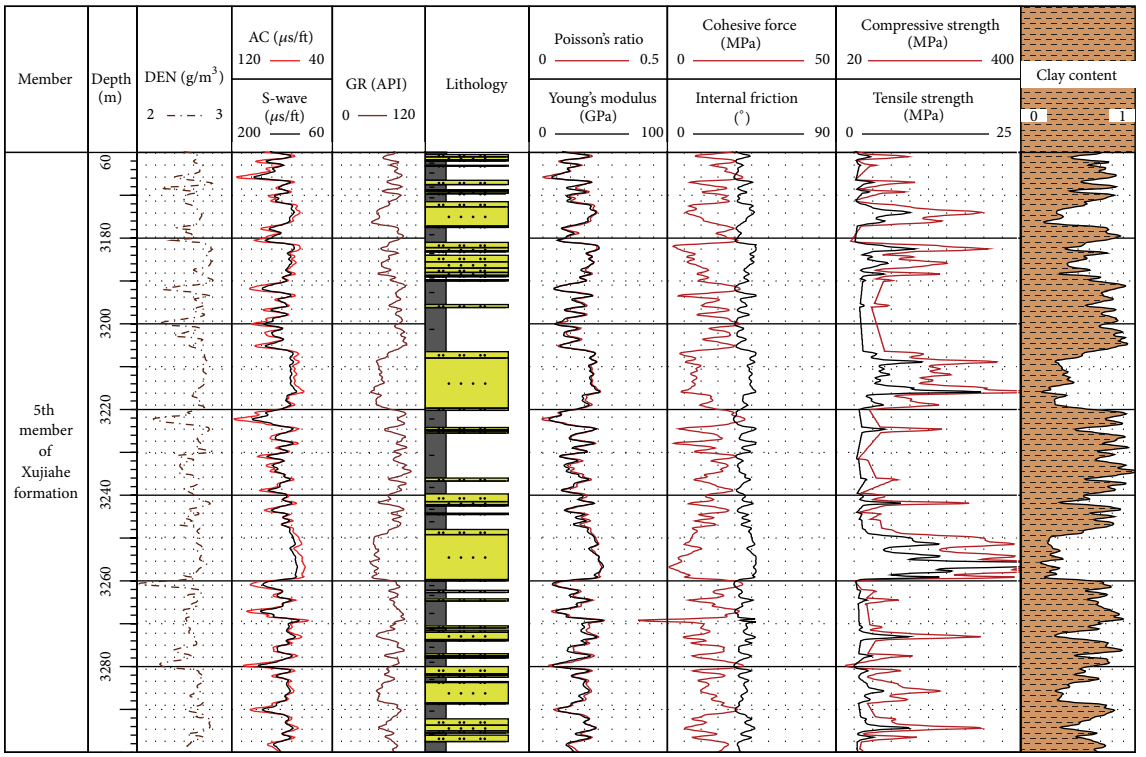

Figure 10: The rock mechanics logging interpretation longitudinal section.

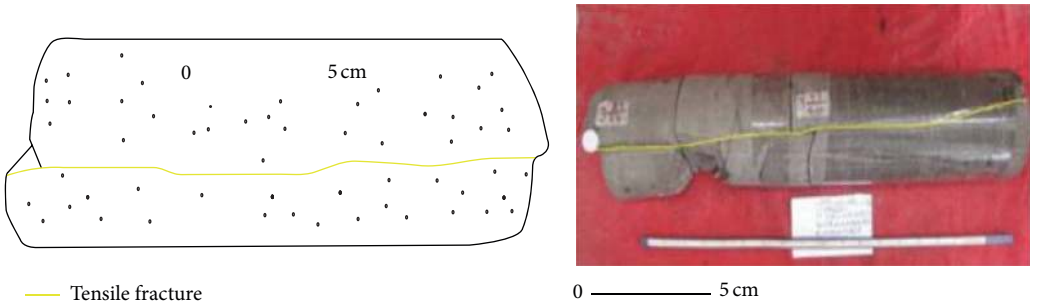

(a) Typical tensile fractures in core (XYHF-1, 3044.5–3048.42 m)

(b) Typical tensile fractures in core (XYHF-1, 3032.81–3033.11 m)

Figure 11: Typical natural fractures.

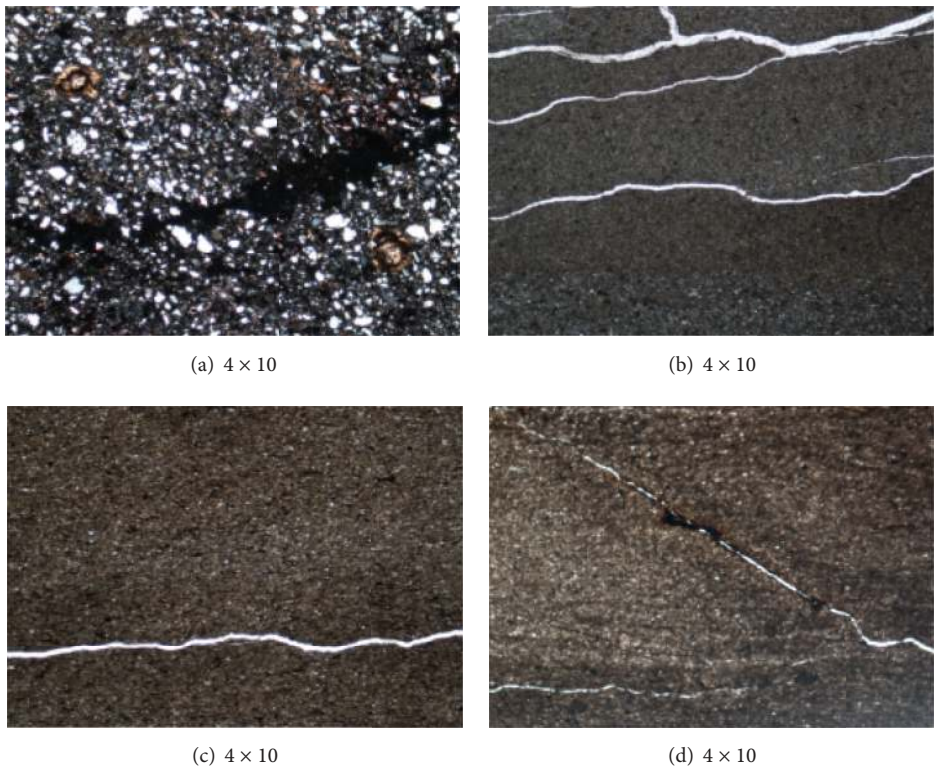

(a) 4 × 10 (b) 4 × 10

(c) 4 × 10 (d) 4 × 10

Figure 12: The microscopic failures of the samples in the cross section: (a) tensile fractures in sandstone, (b) shear fractures in mudstone, (c) tensile fractures in mudstone, and (d) shear fracture and tensile fracture in mudstone.

well (Figure 12(b)). Moreover, there were also some tensile fractures in the mudstone (Figures 12(c) and 12(d)).

After testing and measuring the statistics of approximately 8 sample fractures, results indicate that there are two types of fractures: shear fractures and tensile fractures. Approximately 74.1% of the fractures in sandstone are tensile fractures, but only 25.9% of the fractures are shear fractures. In contrast, 35.1% of fractures in mudstone are shear fractures and 64.9% of the fractures are tensile fractures (Figure 13). Natural fractures from core samples are taken into consideration. Natural fracture statistics show the same phenomenon. Moreover, it is known that sandstones show strong rigidity, while mudstones show plasticity. Following conclusions can be drawn:

(1) In the compressive stress zone, tensile fractures are generated easily in the sandstone.

(2) Mudstone shows strong plasticity. Tensile stress derived from bending structures can lead to rock deformation; thus, shear fractures mainly develop in mudstone.

(3) Most tensile fractures in the mudstone originate in the sandstone and then break the barrier into the neighboring mudstone layer.

Finally, with the conclusions above and based on statistics combined with structure stress, a fracture deformation model can be developed (Figure 14).

7. Conclusions

Firstly, using the distinct characteristics of sandstone and mudstone in combination with the conversion formula of dynamic and static modulus, series of such variables as compressive strength, tensile strength, and shear strength were obtained.

Secondly, the logging interpretation section of the fifth member of the Xujiahe formation in the Xinchang gas field was established. The comparison of measured data and log-calculated data indicates that the log interpretation of rock mechanics in this formation is reliable for compressive strength, cohesive force, and Poisson's ratio.

Finally, natural fractures in downhole cores and rock microscopic failure in the samples in the cross section show that tensile fractures were mainly found in sandstone and shear fractures can be found in both mudstone and sandstone. Based on different elasticity and plasticity in different rocks, as well as the characteristics of natural fractures, the fracture propagation model was established.

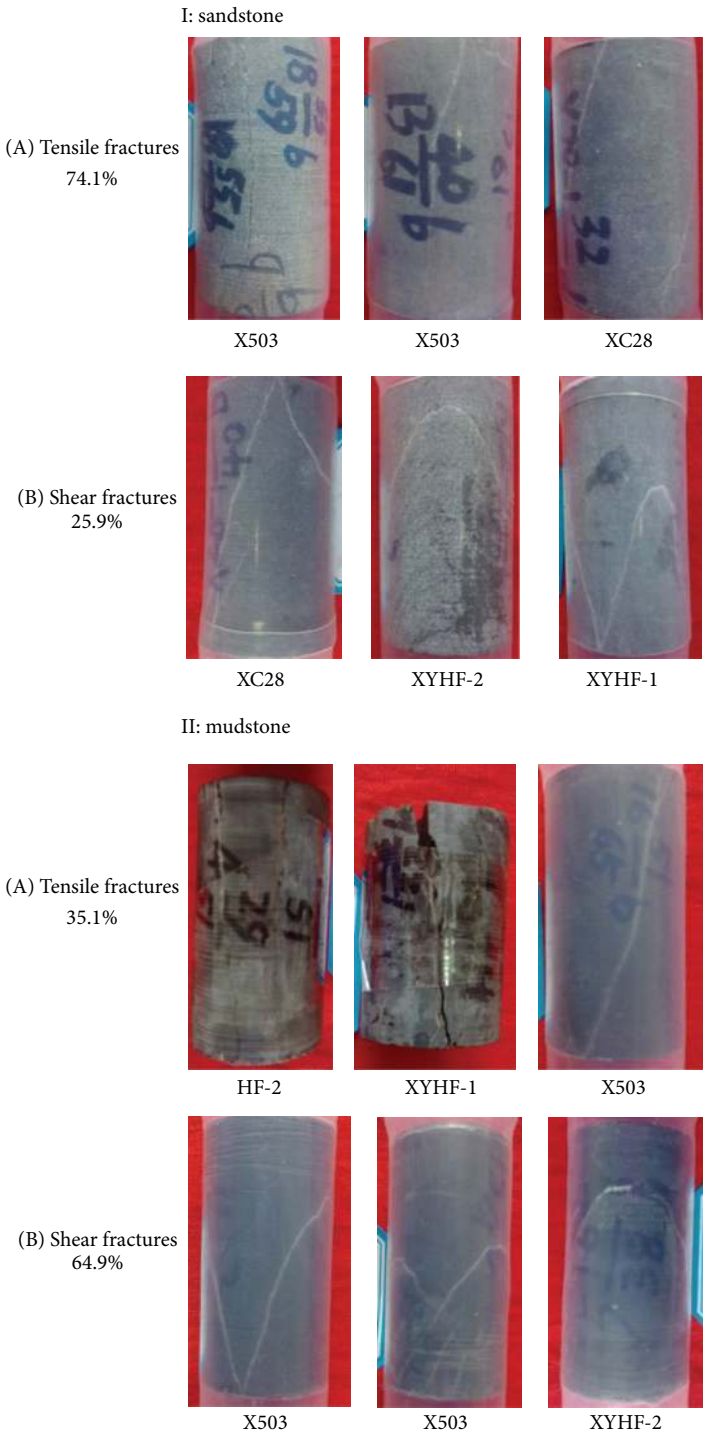

Figure 13: Fractures after the experiment.

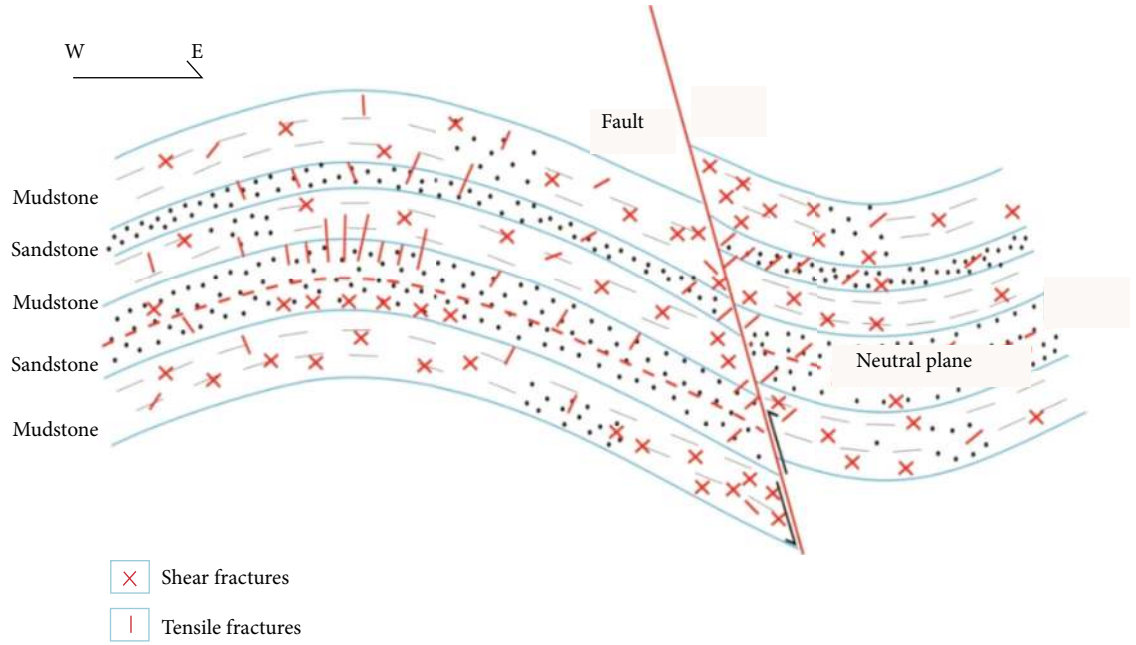

Figure 14: Fracture and deformation model.

Competing Interests

The authors declare that they have no competing interests.

Acknowledgments

The authors would like to thank SINOPEC for providing the reservoir data to make this study possible. The authors also thank the National Natural Science Foundation of China (no. 41572130) and the China Postdoctoral Science Foundation (no. 20110491740) for financial support.

References

[1] L. Baoping and B. Hongzhi, "Advances in calculation methods for rock mechanics parameters," *Petroleum Drilling Techniques*, vol. 33, no. 5, pp. 44–47, 2005.

[2] J. Guo and Y. Liu, "A comprehensive model for simulating fracturing fluid leakoff in natural fractures," *Journal of Natural Gas Science and Engineering*, vol. 21, pp. 9770–985, 2014.

[3] C. Chang, M. D. Zoback, and A. Khaksar, "Empirical relations between rock strength and physical properties in sedimentary rocks," *Journal of Petroleum Science and Engineering*, vol. 51, no. 3, pp. 223–237, 2006.

[4] A. Abdulraheem, M. Ahmed, A. Vantala, and T. Parvez, "Prediction rock mechanical parameters for hydrocarbon reservoirs using different artificial intelligence techniques," SPE Paper 126094, 2009.

[5] N. A. Al-Shayea, "Effects of testing methods and conditions on the elastic properties of limestone rock," *Engineering Geology*, vol. 74, no. 1-2, pp. 139–156, 2004.

[6] S. Yuming and L. Guowei, "Experimental study on dynamic and static parameters of rocks under formation conditions," *Journal of Chengdu College Geology of Technology*, vol. 27, no. 3, pp. 249–255, 2000.

[7] Z. Wen, *Evaluation Methods of Fracture Reservoir in Oil & Gas Reservoir*, Sichuan Science and Technology Press, Chengdu, China, 1998.

[8] Z. Baoping and M. J. Economides, *Reservoir Stimulation*, Petroleum Industry Press, Beijing, China, 3rd edition, 2002.

[9] R. Ranjbar-Karami, A. kadkhodaie-Ilkhchi, and M. Shiri, "A modified fuzzy inference system for estimation of the static rock elastic properties: a case study from the Kangan and Dalan gas reservoirs, South Pars gas field, the Persian Gulf," *Journal of Natural Gas Science and Engineering*, vol. 21, pp. 962–976, 2014.

[10] E. Fjær, R. M. Holt, P. Horsrud, A. M. Raaen, and R. Risnes, *Petroleum Related Rock Mechanics*, vol. 53, 2nd edition, 2008.

[11] G. Mavko, T. Mukerji, and J. Dvorkin, *The Rock Physics Handbook: Tools for Seismic Analysis in Porous Media*, Cambridge University Press, Cambridge, UK, 2nd edition, 2009.

[12] M. R. J. Wyllie, G. H. F. Gardner, and A. R. Gregory, "Studies of elastic wave attenuation in porous media," *Geophysics*, vol. 27, no. 5, pp. 569–589, 1963.

[13] P. Horsrud, "Estimating mechanical properties of shale from empirical correlations," *SPE Drilling and Completion*, vol. 16, no. 2, pp. 68–73, 2001.

[14] C. Chang, "Expirical rock strength logging in boreholes penetrating sedimentary formations," *Chungnam National University, Daejeon, Geology and Earth Science*, vol. 7, no. 3, pp. 174–183, 2004.

[15] M. Farrokhrouz, M. R. Asef, and R. Kharrat, "Empirical estimation of uniaxial compressive strength of shale formations," *Geophysics*, vol. 79, no. 4, pp. 227–233, 2014.

[16] Z. Dawei, L. Yuxi, Z. Jinchuan et al., *National-Wide Shale Gas Potential Survey and Assessment*, Geological Publishing House, Beijing, China, 2012.

[17] J. Guo, Q. Lu, H. Zhu, Y. Wang, and L. Ma, "Perforating cluster space optimization method of horizontal well multi-stage fracturing in extremely thick unconventional gas reservoir," *Journal of Natural Gas Science and Engineering*, vol. 26, pp. 1648–1662, 2015.

[18] B. Amadei and O. Stephansson, *Rock Stress and Its Measurement*, Chapman & Hall, London, UK, 1997.

[19] M. D. Zoback and J. H. Healy, "In situ stress measurements to 3.5 km depth in the Cajon Pass Scientific Research Borehole: implications for the mechanics of crustal faulting," *Journal of Geophysical Research*, vol. 97, no. 4, pp. 5039–5057, 1992.

[20] S. Itou, "Effect of couple stresses on the stress intensity factors for two parallel cracks in an infinite elastic medium under tension," *Mathematical Problems in Engineering*, vol. 2012, Article ID 575891, 14 pages, 2012.

[21] C. A. Barton and M. D. Zoback, "Wellbore imaging technologies applied to reservoir geomechanics and environmental engineering," in *Geological Applications of Well Logs*, M. Lovell and N. Parkinson, Eds., vol. 13 of *AAPG Methods in Exploration*, pp. 229–239, 2002.

[22] L. B. Colmenares and M. D. Zoback, "A statistical evaluation of intact rock failure criteria constrained by polyaxial test data for five different rocks," *International Journal of Rock Mechanics and Mining Sciences*, vol. 39, no. 6, pp. 695–729, 2002.

[23] T. Y. Irfan, "Mineralogy, fabric properties, and classification of weathered granites in Hong Kong," *Quarterly Journal of Engineering Geology*, vol. 29, no. 1, pp. 5–35, 1996.

[24] G. R. Coates and S. A. Denoo, "Mechanical properties program using borehole analysis and Mohr's circle," in *Proceedings of the 22nd Annual Logging Symposium (SPWLA '81)*, Mexico City, Mexico, June 1981.

[25] S. Bruce, "A mechanical stability log," IADC/SPE Paper 19942, Society of Petroleum Engineers, 1990.